

## ICFDP7-2001009

### ANALYSIS OF UNSTABLE BICOMPONENT COOLING LUBRICANT FLOW IN INLET ANNULAR CHANNELS OF THE BTA DRILLS CONSIDERING INTERACTION PROCESSES, THERMAL EFFECT AND HEAT TRANSFER FROM THE BOUNDING SURFACES

**Ashraf S. Ismail**

Assistant Professor,

Department of Engineering Mathematics and Physics,

Faculty of Engineering, Alexandria University,

Alexandria 21544, Egypt.

#### ABSTRACT

The population balance equation based on the interaction processes, i.e. breakage and coalescence of dispersed phase drops, is used to generate the theoretical drop size distributions in the bicomponent mixtures. The turbulence modification of the continuous phase, due to the presence of a dispersed phase, is taken account. The continuity, momentum, energy, and population balance equations are solved numerically to calculate the temperature, holdup and pressure distributions through the inlet annular channel of the BTA drill. The resulting temperature distribution shows that the use of unstable liquid-liquid dispersion as lubricant/coolant will improve the cooling process due to the resultant effect of the interaction processes (breakage and coalescence of drops), and damping of turbulence due to the presence of dispersed phase. In addition, The resulting pressure distribution, in the inlet annular channel, indicates that the lubrication process to the machining zone will be improved too. Since the resultant effect of the interaction processes and damping of turbulence reduce the pressure loss in the annular channel of the BTA drill. Empirical relations are used to calculate the head loss-flow rate response in the chip removal channel. As the metal removal rate increases, the pumping capacity must increase to prevent plugging in the chip removal channel. The flow rate must be adjusted according to the material of the workpiece. The chip particle size and shape, affects the limit deposit velocity. Thus, more research is necessary to find the suitable tool geometry and flow conditions, which give better chip removal condition.

#### NOMENCLATURE

$A(z,u) \delta u$  the number fraction of drops having volumes between  $u$  and  $u+\delta u$  at position  $z$ .

$C_p$  specific heat (J/kg °k)

$d_{pmax}$  maximum drop diameter (m)

$d$  drop diameter (m),  $[d=(6u/\pi)^{1/3}]$

$H$  film thickness (m)

$h_{b,cb}(z,u)$  rate of drop generation by breakage and coalescence, respectively ( $m^{-3}s^{-1}$ )

$h_{b,cd}(z,u)$  rate of drop destruction by breakage and coalescence, respectively ( $m^{-3}s^{-1}$ )

$h_{s,r}$  heat transfer coefficients from stator and rotor surfaces ( $W/m^2 \text{ } ^\circ k$ )

$f_r, f_s$  turbulent friction factors at rotor and stator

$K_x$  dimensionless shear parameter,  $=(K_r+K_s)/2$

$K_r, K_s$  turbulent shear parameters at rotor and stator surfaces

$L$  length of the inlet annular channel (m)

$M$  mass flow rate (kg/s)

$N$  the total number of drops per unit volume of dispersion.

$P$  pressure ( $N/m^2$ )

$P_{in}$  pressure at entrance ( $N/m^2$ )

$Pr$  local Prandtl number

$Q_s$  heat flux from the bounding surfaces ( $W/m^2$ )

$R, Db$  boring bar radius and diameter (m)

$Re_{r,s}$  Reynolds numbers relative to rotor (boring bar) and stator (workpiece)

$Re_o$   $\rho WH/\mu$ , Reynolds number at the entrance of the inlet channel

$RPM$  boring bar RPM

$r_s, r_r$  mean surface roughness at stator and rotor (m)

$T$  temperature ( $^\circ k$ )

$T_{s,r}$  temperature at stator and rotor surfaces ( $^\circ k$ )

$W, U$  mean flow axial and circumferential velocities (m/s)

$x, y, z$   $(0, \pi d)$ ,  $(0, H)$ ,  $(0, L)$ , coordinates defining the flow region.

$\Phi(z)$  holdup

$\Phi_o$  entrance holdup

$\Gamma$  thermal conductivity ( $W/m \text{ } ^\circ k$ )

$\psi$  viscosity temperature coefficient ( $1/^\circ k$ )

$\sigma$	surface tension (N/m)
$\Omega$	angular velocity of boring bar (1/s)
$\rho$	mixture density ( $\text{kg/m}^3$ )
$\mu$	mixture viscosity ( $\text{Ns/m}^2$ )
$\nu$	mixture kinematic viscosity ( $\text{m}^2/\text{s}$ )
$\varepsilon$	energy dissipation rate per unit mass ( $\text{m}^2/\text{s}^3$ )
$\tau_{xy}, \tau_{zy}$	shear stress in x and z directions ( $\text{N/m}^2$ ), respectively.
$\tau_{xy}  ^H$	shear stress on the boring bar surface ( $\text{N/m}^2$ )
$u$	drop volume ( $\text{m}^3$ )
$u_{\max}, u_{\min}$	maximum and minimum drop volumes in the dispersion (m)
<b>Subscripts</b>	
c	continuous phase
d	dispersed phase
i	index defines the axial position
J, K	define the drop classes
o	inlet condition

## INTRODUCTION

The term deep-hole drilling is normally employed when the depth of the hole to be drilled is large compared with diameter of the drill. As the ratio of depth to diameter increases, it becomes increasingly difficult to produce such holes with a twist drill because of the problems involved in getting the coolant to the hole and to flush out the chips from the hole [1]. The BTA deep hole drilling system, Fig.(1), is a single tube system that has become one of the most successful deep hole drilling systems over the last couple decades. This system incorporates a pressure head to force coolant to the cutting edge through the inlet annular channel. The coolant and chips are exhausted from the bore through the I.D. of the boring bar. Due to its excellent machining performance, deep hole drillings are often applied in high precision manufacturing such as the military industry, machine tool and automobile industries [2].

The principal functions of cutting fluids include cooling the cutting tool and the work, lubricating the face of the tool and the chip, and preventing the chip from welding to the cutting edge. The cutting fluid should also provide a flushing action for chip removal. Thus, in addition to the proper feed, cutting speed, and shape of the cutting tool, careful attention should be given to the selection and use of the proper cutting fluid. Cutting fluid prolong tool life, increase the rate of metal removal, aid in producing a finer finish, and enable machining to closer tolerances [3]. For satisfactory tool life, temperature of the cutting fluid should not be permitted to exceed 110°F. The optimum is between 70 and 80 °F [4]. X Li et al. [5] developed a computational method to calculate the temperature distribution throughout the tool, work and chip in machining with coolant. As the knowledge of the influence of cooling, in machining, on the temperature distribution is important in deciding on the best way in which to apply coolant and in considering the design of more efficient coolants.

One of the main problems associated with deep-hole drilling is chip removal from the machining zone. To overcome this problem the machining zone is flooded with the cutting fluid under high pressure. However, this does not always solve the problem of high energy losses that take

place in the hydraulic systems of these drills, which result in a significant drop in the cutting fluid pressure [6]. Astakhov et al. [6-9] conducted their study to increase the effectiveness of the deep hole drilling process. They mentioned that the presence of Taylor vortices in the inlet annular channel causes increased heat exchange between the incoming coolant and outgoing swarf.

It is pointed out that cooling lubricants represent a significant part of the manufacturing costs, and have to be taken into account when examining economics in machining [10].

Oil-in-water (O/W), with water as the continuous phase, is employed as cutting fluid, in metal machining, under circumstances where the high heat capacity of water is beneficial while the rather poor lubricating properties of an O/W emulsion are acceptable. If the rather small viscosity of this emulsion is inadequate for the application yet fire resistance is required, the water-in-oil (W/O) emulsion where the oil is the continuous phase, is often employed [11]. Al-Sharif et al. [11] compared the temperature profile, in the journal bearing, for both pure oil and W/O mixture. They found that the W/O mixture reduces the temperature increase in the film.

Beatty and Hughes [12] studied the turbulent two-phase flow in annular seals. They found that for unchoked two-phase flow through the seal, the fluid temperature decrease, and quality increase. For choked two-phase flow through the seal, the fluid temperature slightly increases and then decreases.

Rajinder Pal [13] observed that in the turbulent regime, the friction factors for the unstable emulsions fall somewhat below those of the stable emulsions. The difference also increases with the increase in the dispersed phase concentration. He explained that this observation is consistent with the proposed mechanism that the turbulence of the carrier fluid of the emulsions (continuous phase) is modified in the presence of dynamic coalescence and breakup processes. The unstable W/O emulsions exhibit much stronger drag reduction activity than the unstable O/W emulsions.

Thus, because of the good lubricating ability, excellent cooling efficiency, nonflammability, low cost, and drag reduction activity under turbulent flow conditions, of the W/O and O/W mixtures, one of them (W/O) is used as cooling lubricant in the present analysis. A mathematical model is proposed, taking account breakage and coalescence of drops (interaction processes), damping of turbulence due to the presence of dispersed phase, thermal effect due to viscous dissipation, and heat transfer from the bounding surfaces.

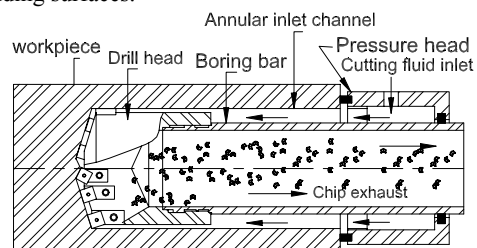


Fig. 1 BTA deep-hole drilling process.

## POPULATION BALANCE MODEL

Considering the control volume in Fig. 2, the population balance model is based on an equation for the continuity of drops numbers in a dispersed phase and is developed from the general conservation equation [14]. For steady state, the population balance equation (PBE) can be written as:

$$\frac{d [W N A(z,u)]}{dz} = h_{bb} - h_{bd} + h_{cb} - h_{cd} \quad (1)$$

The functions  $h_{bb}$ ,  $h_{bd}$ ,  $h_{cb}$ , and  $h_{cd}$  are described in [15]. Solution of the resulting population balance equation, enables prediction of drop size distribution.

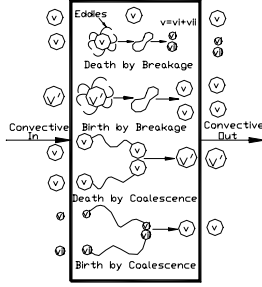


Fig. 2 Control volume

The effective physical properties of the mixture are functions in the local holdup  $\Phi(z)$ , such that

$$\rho(z) = \rho_d \Phi(z) + \rho_c (1 - \Phi(z))$$

$$Cp(z) = Cp_d \Phi(z) + Cp_c (1 - \Phi(z))$$

$$\Gamma(z) = \Gamma_d \Phi(z) + \Gamma_c (1 - \Phi(z))$$

$$\mu(z, T) = \mu_c \left\{ 1 + 2 \Phi(z) \left[ \frac{0.4 + (\mu_d/\mu_c)}{1 + (\mu_d/\mu_c)} \right] \right\}$$

$$\mu_c = \mu_{c0} e^{-\Psi_c (T - T_0)}$$

$$\mu_d = \mu_{d0} e^{-\Psi_d (T - T_0)} \quad (2)$$

## TURBULENCE MODULATION BY DISPERSED PHASE AND BULK-FLOW GOVERNING EQUATIONS

It has been reported in the literature [16] that experiments on two-phase jet flows show that the “damping” of turbulence can be approximated by correlation between mean square velocity fluctuation in turbulence jets in the presence and absence of dispersed phase:

$$u'^2 = \frac{u_0'^2}{(1 + 4 \Phi(z))^2} \quad (3)$$

Thus, in the present analysis, the turbulent stresses are multiplied by a function  $\gamma$  to take into account the damping effect on turbulence by the dispersed phase.

$$\tau(\text{damped}) = \gamma \tau(\text{undamped}) \quad (4)$$

$$\text{where } \gamma = 1/(1 + 4 \Phi(z))^2 \quad (5)$$

Hirs' bulk-flow theory for turbulence in thin film flows is used. The considerations and assumption of a homogeneous mixture for the two-phase region makes Hirs' shear stress model adequate for the proposed two-phase flow model. The turbulent bulk-flow of variable properties is described by the continuity and momentum equations given as [17]:

### Continuity:

$$M = 2 \pi R H \rho W = \text{Constant} \quad (6)$$

### Circumferential Momentum:

$$\tau_{xy} \Big|_0^H = - \frac{\mu}{H} (K_x U - K_r \frac{R \Omega}{2}) = 0 \quad (7)$$

Rearrange Eq.(7) to obtain

$$U = \frac{K_r R \Omega}{2 K_x} \quad (8)$$

### Axial Momentum:

$$\frac{d(\rho H W^2)}{dz} = - H \frac{dP}{dz} + \gamma \tau_{zy} \Big|_0^H \quad (9)$$

where,

$$\tau_{zy} \Big|_0^H = - \frac{\mu (K_r + K_s)}{2 H} W \quad (10)$$

$$K_r = f_r Re_r$$

$$K_s = f_s Re_s$$

$$f_r = a_m \left\{ 1 + \left( \frac{C_m r_r}{H} + \frac{b_m}{Re_r} \right)^e \right\}$$

$$f_s = a_m \left\{ 1 + \left( \frac{C_m r_s}{H} + \frac{b_m}{Re_s} \right)^e \right\}$$

$$a_m = 0.001375 ; b_m = 5 \times 10^5, \quad C_m = 10^4, \quad e = 1/3$$

$$Re_r = \rho H \{(U - \Omega R)^2 + W^2\}^{0.5} / \mu$$

$$Re_s = \rho H \{U^2 + W^2\}^{0.5} / \mu \quad (11)$$

**Energy Equation:**

$$\frac{d(\rho C_p H W T)}{dz} = Q_s + R \Omega \tau_{xy}|^H - U \tau_{xy}|_0^H - W \tau_{zy}|_0^H \quad (12)$$

$$\tau_{xy}|^H = \frac{\mu}{4H} \{ U K_s - (U - R \Omega) K_r \} \quad (13)$$

$$Q_s = h_s(T_s - T) + h_r(T_r - T) \quad (14)$$

$$h_s = 0.5 \rho C_p V_r f_s / Pr^{2/3}$$

$$h_r = 0.5 \rho C_p V_r f_r / Pr^{2/3}$$

$$Pr = C_p \mu / \Gamma \quad (15)$$

$$V_r = \sqrt{U^2 + W^2}$$

**NUMERICAL ANALYSIS**

The numerical analysis are described in [15]. The flow chart in Fig. 3 describes the iterative solution steps. The axial velocity W is calculated from the continuity equation. The pressure distribution is calculated from the axial momentum equation, which can be written as:

$$P_i = P_{i-1} + \frac{\Delta z}{H} [ \gamma \tau_{zyl_0}^H - \frac{d}{dz} (\rho H W^2) ]_i \quad (16)$$

The temperature distribution is calculated from the energy equation, which can be written as:

$$T_{i+1} = T_i + \left( \frac{\Delta z}{H \rho_i W_i C_{p_i}} \right) \{ Q_s - T H \frac{d(\rho W C_p)}{dz} - R \Omega \tau_{xy}|^H - U \tau_{xy}|_0^H - W \tau_{zy}|_0^H \}_i \quad (17)$$

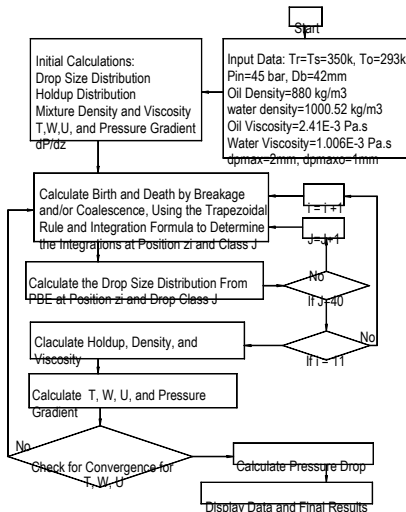


**Fig. 3 Flow chart.**

**TEMPERATURE RISE AND PRESSURE LOSS**

The temperature rise represents the difference between the temperature at the outlet and inlet sections of the annular channel. The total effect of the interaction processes (breakage and coalescence of drops), and damping of turbulence, decreases the temperature rise and the pressure loss through the annular channel and this effect increases as Re<sub>o</sub> increase, H decrease, RPM increase, and Φ<sub>o</sub> increase. This could be concluded from Figs.(4-10) and Figs.(11-13), by comparing the case of considering the interaction processes and damping of turbulence, with the case of neglecting these processes. In Figs.(4-7), the heat transfer from the bounding surfaces (boring bar and workpiece) to the cooling lubricant is neglected (Q<sub>s</sub>=0.0).

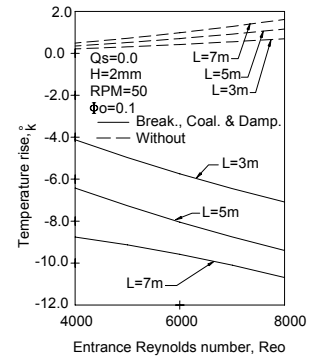


**Fig. 4 Effect of Reo on temperature rise.**

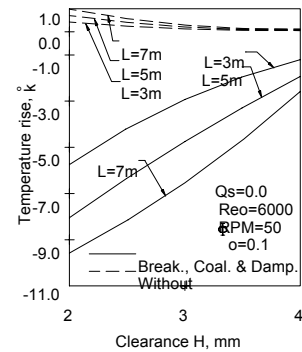


**Fig. 5 Effect of H on temperature rise.**

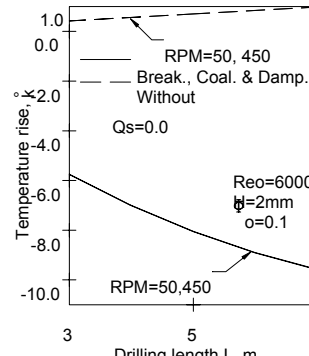


**Fig. 6 Effect of RPM on temperature rise.**

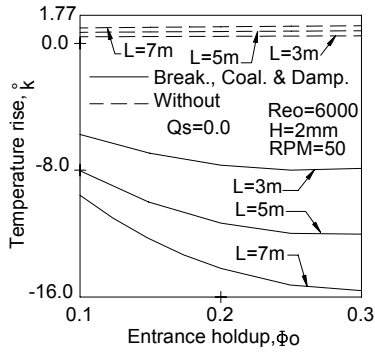


Fig. 7 Effect of  $\Phi_0$  on temperature rise.

In Figs.(8-10),  $Q_s$  is taken account, where  $T_r$  and  $T_s$  are assumed constants ( $T_r=T_s=350^\circ\text{k}$ ). The inlet Temperature  $T_o=293^\circ\text{k}$ . The inlet pressure  $P_{in}=45\text{ bar}$ .

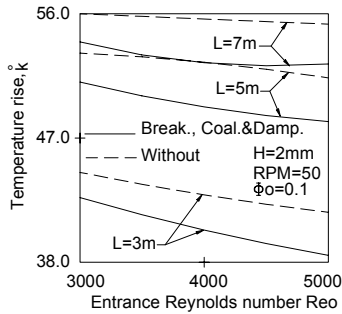


Fig. 8 Effect of  $Re_0$  on temperature rise.

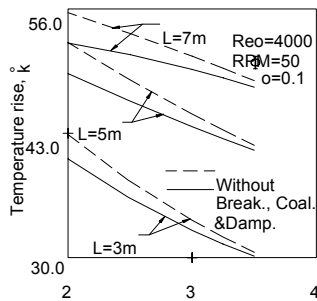


Fig. 9 Effect of  $H$  on temperature rise.

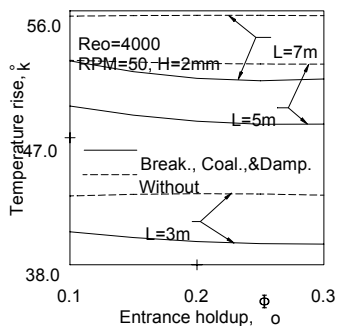


Fig. 10 Effect of  $\Phi_0$  on temperature rise.

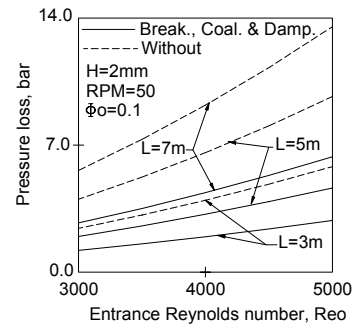


Fig. 11 Effect of  $Re_0$  on pressure loss.

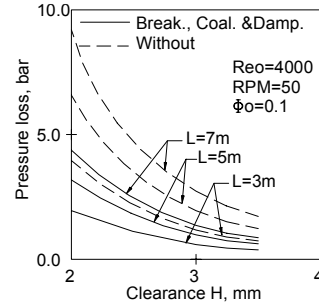


Fig. 12 Effect of  $H$  on pressure loss

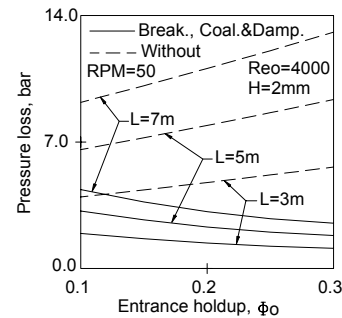


Fig. 13 Effect of  $\Phi_0$  on pressure loss.

## FLOW THROUGH CHIP REMOVAL CHANNEL

Reliable chip removal is one of the most important requirements of deep-hole drilling. In the present study, the flow of the cutting fluid-chip mixture through the chip removal channel is studied using the empirical relations of Swamee and Ojha [1991], and Swamee [1995].

The chip particle morphology and size are affected by several factors such as cutting conditions, cutting fluid properties, and shape of the cutting tool head. Mazurkiewicz et al. [1989] concluded that the use of high-pressure water-jet injection into the tool/chip interface, during metal cutting, creates short curled cool chips, Fig. 14. Crafoord et al. [1999] mentioned that good chip control has a great influence on the tool life, machined surface quality, cutting forces, reliability of the machining process, and productivity. They made an experimental study of the skew cutting of an end of a pipe using a plain high-pressure water jet. The jet was directed perpendicularly to the cutting edge into the tool/chip interface. They show that the chip upcurl radius can be successfully controlled, Fig. 15. In the

present analysis, the chip particle is assumed to be spherical and cylindrical for simplicity.

The cutting fluid-chip mixture flow is treated as a hetero-homogeneous flow. The density and viscosity of the mixture are expressed as:

$$\rho_m = \rho_{ch} C_v + (1-C_v) \rho_{cf} \quad (18)$$

$$\mu_m = \mu_{cf} (1+2.5 C_v) \quad (19)$$

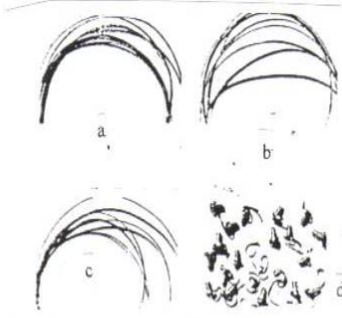


Fig. 14 Chip shapes for orthogonal cutting of UNS 1020 steel at a cutting speed of 180 m/min and feed rate of 0.4 mm/rev; (a) without cooling; (b) with conventional overhead cooling; (c) axiparallel cooling; (d) high-pressure water-jet cooling.

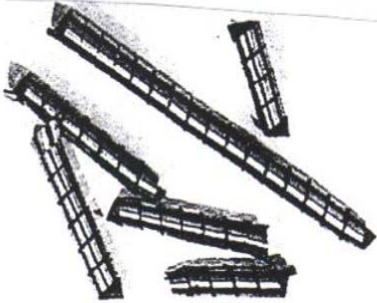


Fig. 15 Chips produced with a feed rate of 0.2 mm/rev (work material: SS2258, SAE52100, commonly, this material produces long and continuous chips).

The deposit velocity for suspension containing multi-sized particles is generally estimated by assuming a mean particle size to the suspension. Spels [1995] used  $d_{85}$  as particle size to be used in his correlation. In the present study,  $d_{85}$  is used to represent the particle diameter such that 85% by weight of the particles are smaller than  $d_{85}$ .

The head loss for the flow of fluid in a circular pipe with heterogeneous suspension of sediment particles, are [19]:

$$h_f = \frac{f L W^2}{2 g D} + \frac{81 (S-1) C_v f L \sqrt{(S-1) g D}}{2 C_D^{0.75} W} \quad (20)$$

in which  $L$  = pipe length;  $W$  = average velocity of flow;  $g$  = gravitational acceleration;  $D$  = pipe diameter;  $C_v$  = volumetric sediment concentration;  $S$  = ratio of mass

densities of particle and fluid;  $CD$  = drag coefficient of particle; and  $f$  = friction factor for sediment fluid mixture, which can be determined by the following equation [19]:

$$f = \left\{ \left( \frac{\epsilon}{Re} \right)^8 + 9.5 \left[ \ln \left( \frac{\epsilon}{3.7D} + \frac{5.74}{Re^{0.9}} \right) - \left( \frac{2500}{Re} \right)^6 \right]^{-16} \right\}^{0.125} \quad (21)$$

in which  $\epsilon$  = average height of the roughness projections of pipe wall; and  $Re$  = Reynolds number defined by

$$Re = \frac{W D}{\nu_m} \quad (22)$$

in which  $\nu_m$  = kinematic viscosity of fluid sediment mixture. Eq. (21) is valid for laminar flow as well as turbulent flow and the transition in between. For a spherical particle of diameter  $d$ , the drag coefficient of particle is [18]:

$$C_D = 0.5 \left\{ 16 \left[ \left( \frac{24}{Rs} \right)^{1.6} + \left( \frac{130}{Rs} \right)^{0.72} \right] 2.5 + \frac{40000}{\left[ \left( \frac{40000}{Rs} \right)^2 + 1 \right]^{0.25}} \right\}^{0.25} \quad (23)$$

in which  $Rs$  = sediment particle Reynolds number given by

$$Rs = \frac{\omega d}{\nu_m} \quad (24)$$

in which  $\omega$  = fall velocity of sediment particle. Eq. (23) is valid for  $Rs \leq 1.5 \times 10^5$ . The fall velocity,  $\omega$ , of a spherical particle is [18]:

$$\omega = \left( \sqrt{(S-1) g d} \right) \left\{ \left[ (18 \nu')^2 + (72 \nu')^{0.54} \right]^5 + \left[ (10^8 \nu')^{1.7} + 1.43 \times 10^6 \right]^{-0.346} \right\}^{-0.1} \quad (25)$$

where

$$\nu' = \frac{\nu_m}{d \sqrt{(S-1) g d}} \quad (26)$$

Eq. (25) is valid for  $\nu' \geq 4 \times 10^{-5}$ . The mixture velocity is written as:

$$W = \frac{4 (Q_f + Q_{ch})}{\pi D^2} \quad (27)$$

Where  $Q_f$  and  $Q_{ch}$  are the cutting fluid and chip particle volumetric flow rates, respectively. The volumetric concentration,  $C_v$ , of the chip particles is defined as:

$$C_v = \frac{Q_{ch}}{Q_r + Q_{ch}} \quad (28)$$

For a nonspherical particle of volume  $u$ , the nominal diameter  $d_n$  is defined [18]

$$d_n = (6u/\pi)^{1/3} \quad (29)$$

The shape factor of a nonspherical particle  $\beta$  is expressed

$$\beta = \frac{c}{\sqrt{ab}} \quad (30)$$

in which  $a$ ,  $b$ , and  $c$  = lengths of the three principal axes of the particle in decreasing order of magnitude. The parameter  $\beta$  is zero for a two-dimensional plate and unity for a sphere. For nonspherical particle, the following equations are used [18]:

$$C_D = \left[ \frac{48.5}{(1+4.5\beta^{0.35})^{0.8} R_s^{0.64}} + \left( \frac{R_s}{R_s+100+1000\beta} \right)^{0.32} \frac{1}{(\beta^{18} + 1.05\beta^{0.8})} \right]^{1.25} \quad (31)$$

$$\omega = (\sqrt{(S-1)g} d_n) \left\{ \frac{44.84 v'^{0.667}}{(1+4.5\beta^{0.35})^{0.833}} + \frac{0.866}{(\beta^{18} + 1.05\beta^{0.8} + 34.0 v'^{1.3})^{0.625}} \right\}^{-1} \quad (32)$$

Eq. (32) is valid for  $v' \geq (1.8 \times 10^{-4})/\beta$ .

### DESIGN CONSIDERATIONS FOR CHIP REMOVAL CHANNEL

If the selected cutting fluid flow rate is too small, the formed chips would accumulate and block the chip removal process. On the other hand, if it is too high, there is large head loss amounting to a high cost of pumping. The desired state of suspension is very essential for the design of the chip removal channel and the determination of the necessary power input. Figs. (16-19) give the head loss per unit length-flow rate response for the flow of heterogeneous suspension of chip particles, for different values of  $S$ ,  $C_v$ ,  $d_{85}$ , and  $\beta$ . The velocity at minimum in the head loss-flow rate curve is called the "limit deposit velocity". The dashed line in Figs. (16-19) intersects the curves at the points of limit deposit velocity.

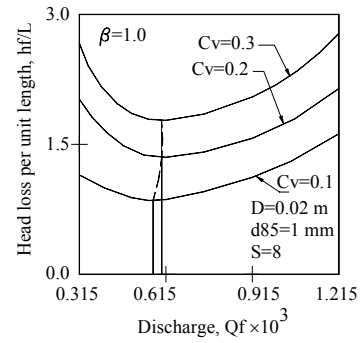


Fig. 16 Effect of  $C_v$  on head loss.

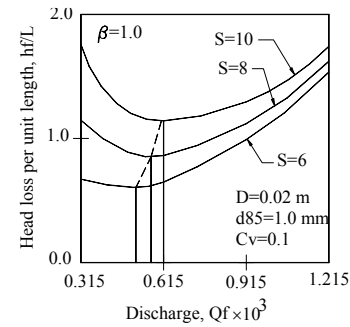


Fig. 17 Effect of  $S$  on head loss.

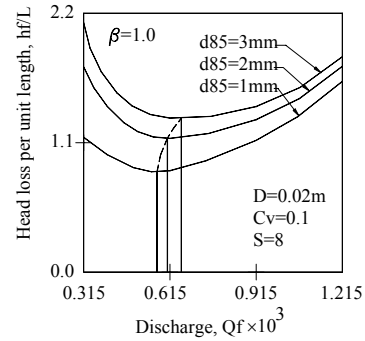


Fig. 18 Effect of  $d_{85}$  on head loss.

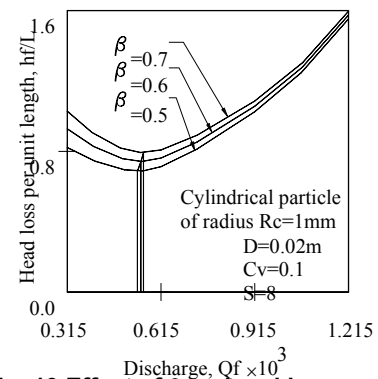


Fig. 19 Effect of  $\beta$  on head loss.

If the velocity is reduced beyond the limit deposit velocity, a bed of chip particles begins to build up in the channel and head loss increases due to the restriction of the available flow area. At the higher flow rates, i.e. the concentration

gradient of the chip particles becomes less pronounced and the system tends towards homogeneity. As the velocity of the cutting fluid increases, the turbulence intensity will increase and the eddies will have sufficient energy to suspend the particles and overcome the gravity forces.

## CONCLUSIONS

The resulting temperature distribution shows that the use of unstable liquid-liquid dispersion as lubricant/coolant will improve the cooling process due to the resultant effect of the interaction processes (breakage and coalescence of drops), and damping of turbulence due to the presence of dispersed phase. The reduction in the temperature rise through the annular channel, due to interaction processes and damping of turbulence, increases as entrance Reynolds number increases, clearance decrease, drilling length increase, and entrance holdup increase. In addition, The resulting pressure distribution, in the inlet annular channel, indicates that the lubrication process to the machining zone will be improved too. Since the resultant effect of the interaction processes and damping of turbulence reduces the pressure loss in the annular channel of the BTA drill.

As the metal removal rate increases, the pumping capacity must increase to prevent plugging in the chip removal channel. The flow rate must be adjusted according to the material of the workpiece. The chip particle size and shape, affects the limit deposit velocity. Thus, more research is necessary to find the suitable tool geometry and flow conditions, which give better chip removal condition.

## REFERENCES

[1] HMT Bangalore, 1994, "Production Technology", Tata McGraw-Hill Publishing Company Limited, New Delhi, Tenth Reprint, Section 6, pp. 161-184.

[2] Chin, J., Hsieh, C., and Lee, L., 1996, "The Shaft Behavior of BTA Deep Hole Drilling Tool", *Int. J. Mech. Sci.*, vol. 38, No. 5, pp. 461-482.

[3] McCarthy, W.J., and Repp, V.E., 1979, "Machine Tool Technology", McKnight Publishing Company, Bloomington, Illinois, Fourth Edition, Unit 116, pp.449-465.

[4] ASME Research Committee on Metal Cutting Data and Bibliography Manual on Cutting of Metals With Single-Point Tools, The American Society of Mechanical Engineers, Second Edition, Part III, Chapter 6, pp.185 (1952).

[5] X Li, Kopalinsky, E.M., and Oxley, P.L.B. A, 1995, "Numerical Method for Determining Temperature Distributions in Machining With Coolant- Part 1: Modelling the Process", *Proc. Instn. Mech. Engrs., Part B: Journal of Engineering Manufacture*, 209, 33-43.

[6] Astakhov, V.P., Subramanya, P.S., and Osman, M.O.M., 1996, "On The Design of Ejectors for Deep Hole Machining," *Int. J. Mach. Tools Manufact.*, vol. 36, No. 2, pp. 155-171.

[7] Astakhov, V.P., Subramanya, P.S. and Osman, M.O.M., 1995, "An investigation of the cutting fluid flow in self-piloting drills," *Int. J. Mach. Tools Manufact.*, Vol. 35(4), pp. 547-563.

[8] Astakhov, V.P., Subramanya, P.S., and Osman, M.O.M., 1995, "Theoretical and experimental

investigations of coolant flow in inlet channels of the BTA and ejector drills", *Proc. Instn. Mech. Engrs., Part B: Journal of Engineering Manufacture*, vol. 209, pp. 211-220.

[9] Astakhov, V.P., Abi Karam, S., and Osman, M.O.M., 1998, "The Correlation Between the Cutting Fluid Distribution and the Topography of Tool Wear in BTA Drilling", *ASME Journal of Manufacturing Science and Engineering*, Vol. 120, pp. 820-822.

[10] Brinksmeier, E., Walter, A., Janssen, R., and Diersen, 1999, "Aspects of Cooling Lubrication reduction in machining advanced materials," *Proc. Instn. Mech. Engrs.*, vol. 213, part B, pp. 769-778.

[11] Al-Sharif, A., Chamniprasart, K., Rajagopal, K.R., and Szeri, A.Z., 1993, "Lubrication With Binary Mixtures: Liquid-Liquid Emulsion", *ASME Journal of Tribology*, Vol. 115, pp. 46-55.

[12] Beatty, P.A., and Hughes, W.F., 1986, "Turbulent Two-Phase Flow in Annular Seals", *ASLE 41<sup>st</sup> Annual Meeting in Toronto, Ontario, Canada*, May 12-15.

[13] Rajinder Pal, 1993, "Pipeline Flow of Unstable and Surfactant-Stabilized Emulsions", *AICHE Journal*, vol. 39, No.11, pp.1754-1764.

[14] Ramkrishna, D., 1985, "The Status of Population Balances", *Reviews in Chemical Engineering*, vol. 3, No.1, pp. 49-95.

[15] Ismail, A.S., 2001, "Analysis of Unstable Bicomponent Cooling Lubricant Flow in Inlet Annular Channels of the BTA Drills in the Presence of Dynamic Breakage and Coalescence Processes", Submitted for presentation in the Seventh International Congress on Fluid Dynamics and Propulsion (ICFDP7), December 19-21, 2001, Sharm El-Sheikh, Sinai, Egypt.

[16] Coualoglou, C.A., and Tavlarides L.L., 1977, "Description of Interaction Processes in Agitated Liquid-Liquid Dispersions," *Chemical Engineering Science*, Vol. 32, pp. 1289-1297.

[17] Arauz, G. L. and San Andres, L., 1998, "Analysis of Two-Phase Flow in Cryogenic Damper Seals-Part I: Theoretical Model," *ASME Journal of Tribology*, Vol. 120, pp. 221-227.

[18] Swamee, P.K. and Ojha, C.S.P., 1991, "Drag Coefficient and Fall Velocity of Nonspherical Particles", *J. of Hydraulic Engineering*, ASCE, Vol. 117, No. 5, pp. 660-667.

[19] Swamee, P.K., 1995, "Design of Sediment-Transporting Pipeline", *J. of Hydraulic Engineering*, ASCE, Vol. 121, No. 1, pp. 72-76.

[20] Mazurkiewicz, M., Kubala, Z., and Chow, J., 1989, "Metal Machining With High-Pressure Water-Jet Cooling Assistance- A new Possibility", *ASME J. of Engineering for Industry*, Vol. 111, pp.7-12.

[21] Crafoord, R., Kaminski, J., Lagerberg, S., Ljungkrona, O., and Wretland, A., 1999, "Chip Control in Tube Turning Using A high-Pressure Water Jet", *Proc. Instn. Mech. Engrs.*, Vol. 213, Part B, pp. 761-767.

[22] Spells, K.E., 1995, "Correlation for Use in Transport of Aqueous Suspensions of Fine Solids Through Pipes", *Trans. Instn. Chem. Eng.*, Vol. 33, pp. 79-84.